

FLUORESCENCE DIFFUSE OPTICAL TOMOGRAPHY: A SIMULATION-BASED STUDY COMPARING TIME-RESOLVED AND CONTINUOUS WAVE RECONSTRUCTIONS PERFORMANCES

Nicolas Ducros,^{1,2*} Anabela da Silva,¹ Jean-Marc Dinten,¹ and Françoise Peyrin², IEEE Member

¹Micro Technologies for Biology and Healthcare Division, CEA-LETI MINATEC, 17 rue des Martyrs, 38054 Grenoble, France

²CREATIS -UMR CNRS 5220 -INSERM U630, INSA Lyon, Bât. Blaise Pascal, 69621 Villeurbanne Cedex, France.

*corresponding author : nicolas.ducros@cea.fr

ABSTRACT

The present paper is devoted to a comparison between time-resolved fluorescence diffuse optical tomography and continuous wave fluorescence diffuse optical tomography. Both of these techniques aim at reconstructing 3D biodistribution of fluorescent markers embedded in biological tissues. The study is restricted in the time domain to the exploitation of the first three temporal moments of measurements. The temporal benefits in terms of reconstruction have been shown to depend strongly on the optical parameters of the medium investigated as well as the fluorescence lifetime.

Index Terms— Fluorescence Diffuse Optical Tomography; Time-resolved imaging, Inverse Problems.

1. INTRODUCTION

Light imaging techniques in the near-infrared (NIR) window benefit from low tissue absorption. Since photons can propagate over several centimeters within biological tissues in NIR wavelength, NIR photons can be used to explore the inner tissue structure [1]. Recently, the development of NIR fluorescent markers has led to a new imaging technique, namely fluorescence diffuse optical tomography (FDOT), able to determine the 3D local concentrations of fluorescent agents. Such markers have been increasingly studied in the last years. Some of them have been designed to fix on specific proteins then behaving as molecular probes. Others called activable become fluorescent only in the vicinity of a given protein [2]. Parallely, the emergence of quantum dots is also promising to enlarge the potential uses of fluorescent markers [3]. Monitoring such markers in vivo could give rise to the collection of a large amount of functional information. In this context, FDOT can play a significant role in small animal imaging as well as in drug discovery and delivery.

The FDOT is based on the ability of fluorescent markers to absorb incident light and as a response to emit light at a longer wavelength [4]. Considering a set of external light excitations and a resulting set of external fluorescent light detections, a tomographic scheme can be applied to a medium injected with fluorescence markers to recover local concentration in fluorescent markers. This reconstruction implies the use and the inversion of an appropriate model accounting for both the photon propagation and the fluorescence phenomena.

Continuous wave (CW) FDOT and time-resolved (TR) FDOT differ from the excitation-detection mode used. CW FDOT is based on the measurement of the attenuation of a steady state excitation light. TR FDOT is based on the temporal measurement of the distortion of an excitation pulse of light. The latter excitation mode is regarded as the way to maximize the amount of information collected from the fluorescence measurements and also as a way to reconstruct deeply embedded markers. The focus was initially made on early arriving photons [5] of temporal signals. However, that approach suffers from low signal to noise ratio and provides poor depth resolution. More recently, the trend is to exploit signatures of full time-resolved fluorescence signals [6], [7], [8]. Among them, the Laplace transform of the TR fluorescence signals [7] and the temporal moments of the fluorescence signals have been investigated by several authors [8-10]. The moments are of particular interest since they allow a physical interpretation in terms of number of photons, time of flight, variance, etc.

In the present paper, we propose to evaluate the benefit of using TR fluorescence signals reduced to their moments rather than the CW, considered as the gold standard, according to optical considerations (absorption, diffusion and lifetime). In particular, we introduce a new criterion combining the optical properties of the medium and the fluorescence lifetime, useful in the interpretation of the results.

2. THEORY

2.1. Light Propagation

The NIR light propagation within a turbid media such as biological tissues has been successfully modeled by the diffusion theory [1]. Indeed, the photons density $\phi(\mathbf{r}, t)$ (W.cm^{-2}) at position \mathbf{r} and time t , in a medium wherein the scattering probability is much larger than the absorption, satisfies the photon diffusion equation. In particular, regarding a light pulse emitted at position \mathbf{r}' and time zero into an optically homogeneous medium, it can be stated that:

$$\frac{1}{v} \frac{\partial}{\partial t} \phi(\mathbf{r}, t) - D \nabla^2 \phi(\mathbf{r}, t) + \mu_a \phi(\mathbf{r}, t) = S \delta(\mathbf{r} - \mathbf{r}', t) \quad (1)$$

$v = c/n$ (cm.ns^{-1}) is the speed of light in the medium of refractive index n . δ represents the Dirac function. S is the intensity of the input signal (W.cm^{-3}). $D = 1/3\mu'_s$ (cm) as recommended in [11] is the diffusion constant. μ'_s (cm^{-1}) is known as the reduced scattering coefficient and μ_a is the absorption coefficient (cm^{-1}).

2.2. Fluorescence

The fluorescence signal U_{fl} , measured in FDOT, results from a three-stage process. First, light emitted at the wavelength λ_{em} propagates through the medium from the excitation point to a fluorescent marker. Second, the fluorescent marker absorbs excitation light and reemits fluorescence light at the wavelength $\lambda_{ex} < \lambda_{em}$. Third, the fluorescence light propagates through the medium from the fluorescence marker to the detector. This process can be modeled in the time domain as [4] :

$$U_{fl}(\mathbf{r}_s, \mathbf{r}_d, t) = A \int \phi_{ex}(\mathbf{r}_s, \mathbf{r}, t) *_t F(\mathbf{r}, t) *_t \phi_{em}(\mathbf{r}, \mathbf{r}_d, t) d^3r, \quad (2)$$

where \mathbf{r}_s and \mathbf{r}_d are respectively the positions of the excitation and detection points. A is a constant taking into account experimental parameters (such as transmission of filters, neutral densities, detectors quantum efficiencies, etc). The integration is performed all over the diffusing medium and $*$ _{*t*} denotes the time convolution operator. The subscript *ex* and *em* indicates whether the photon densities ϕ are to be considered at the excitation wavelength λ_{ex} or emission wavelength λ_{em} . The pulse response $F(\mathbf{r}, t)$ of the fluorescent marker at position \mathbf{r} is classically modeled by the exponential decay characterized by the lifetime τ (ns) :

$$F(\mathbf{r}, t) = \eta c(\mathbf{r}) \frac{e^{-t/\tau}}{\tau}, \quad (3)$$

$c(\mathbf{r})$ (μM) is the marker concentration at position \mathbf{r} and η (-) is the quantum yield of fluorescence.

2.3. Forward and Inverse Problems

Let us consider medium Ω containing embedded fluorescent markers. We consider S distinct excitation positions \mathbf{r}_{si} ($1 < i < S$) and D distinct detectors positions \mathbf{r}_{dj} ($1 < j < D$). Discretizing Ω in N voxels centered on \mathbf{r}_k ($1 < k < N$), the integral in (2) can be rewritten as a sum. Then, regarding the three first order temporal moments (noted m_0 , m_1 and m_2) of the fluorescence signals, it has been shown that the inner fluorophores concentration vector c is a linearly related to the peripheral moment measurement vector m [12]. Applying this result to our problem leads to the following formulation:

$$\begin{bmatrix} m_0(\mathbf{r}_{s1}, \mathbf{r}_{d1}) \\ \vdots \\ m_0(\mathbf{r}_{si}, \mathbf{r}_{dj}) m_1(\mathbf{r}_{si}, \mathbf{r}_{dj}) \\ \vdots \\ m_0(\mathbf{r}_{sS}, \mathbf{r}_{dD}) m_2(\mathbf{r}_{sS}, \mathbf{r}_{dD}) \end{bmatrix} = W(\mathbf{r}_s, \mathbf{r}, \mathbf{r}_d) \begin{bmatrix} c(\mathbf{r}_1) \\ \vdots \\ c(\mathbf{r}_k) \\ \vdots \\ c(\mathbf{r}_N) \end{bmatrix}. \quad (4)$$

The $3.S.D \times N$ weight matrix $W(\mathbf{r}_s, \mathbf{r}, \mathbf{r}_d)$ is a function of the first three moments of the photon densities $\phi_{ex}(\mathbf{r}_s, \mathbf{r}, t)$ and $\phi_{em}(\mathbf{r}, \mathbf{r}_d, t)$ expressed in (2), and given by the resolution of (1) with optical properties expressed at each wavelength. The measurement vector M can be constructed considering the following temporal moments:

$$\begin{aligned} m_0(\mathbf{r}_s, \mathbf{r}_d) &= \int U_{fl}(\mathbf{r}_s, \mathbf{r}_d, t) dt, \\ m_1(\mathbf{r}_s, \mathbf{r}_d) &= \frac{1}{m_0(\mathbf{r}_s, \mathbf{r}_d)} \int U_{fl}(\mathbf{r}_s, \mathbf{r}_d, t) t dt, \\ m_2(\mathbf{r}_s, \mathbf{r}_d) &= \frac{1}{m_0(\mathbf{r}_s, \mathbf{r}_d)} \int U_{fl}(\mathbf{r}_s, \mathbf{r}_d, t) t^2 dt, \end{aligned} \quad (5)$$

It is important to note here that the formulation (4) enfold the formulation derived in Continuous Wave (CW) illumination problems. Indeed, zero order moments of the fluorescence signals are equivalent to intensities measured in CW. Hence, equation (4) can be seen as the temporal extension of the continuous case.

The issue of the inverse problem is to retrieve the concentration vector C by measuring moments M and calculating the weight matrix W . This implies the inversion of the system (4). The algebraic techniques and among them the algebraic reconstruction technique (ART) are well known in the biomedical community. ART has already

shown its capability in diffuse optical imaging problems [6] and will be used here to invert (4) with a positivity constraint.

3. MATERIAL AND METHOD

3.1. Synthetic phantom description

In the following, we will hypothesize that the optical properties of the medium are the same at both the excitation and emission wavelengths. This is consistent with most of fluorescent markers used within biological tissue. Homogeneous infinite medium phantoms are considered, presenting different absorption coefficients μ_a , different reduced scattering coefficients μ'_s and a refractive index n set to 1.4 (see Table 1 for details). Each medium is probed by 25 source points and 25 detector points. Sources and detectors are evenly arranged in two square grids of side 5 cm. The two grids are 6 cm apart. Three fluorescent inclusions with varying lifetimes τ are embedded into the phantoms. We consider also a fluorescence background with a ratio background/inclusion of 1:10. The phantom is represented in Fig. 1. The values of the varying parameters investigated are given into table 1.

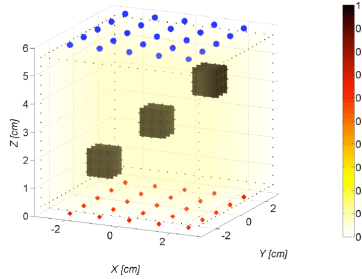


Fig. 1. Synthetic phantom.

τ (ns)	μ_a (cm ⁻¹)	μ'_s (cm ⁻¹)
0.3	0.04	5
0.5	0.08	10
0.9	0.16	20

Table 1. Optical parameters investigated

3.2. Reconstruction

For the reconstruction purpose, the medium is evenly discretized, resulting into 6137 cubic voxels of size (0.3 cm)³. Two types of reconstructions are regarded: the TR reconstruction based on the 3 moments m_0 , m_1 and m_2 and the CW reconstruction. Normalized Born quantities (fluorescence signal normalized by the excitation one) were used in both cases [10].

To carry out the TR reconstruction, we make use of analytical expressions [10]. We calculate the 3 moments of

any of the 625 source-detector couples. The corresponding 1875×6137 TR weight matrix W_{TR} is built up with the same analytical expressions. To carry out the CW reconstruction, we use the equivalence between m_0 and CW measurement. As a result, the 625×6137 CW weight matrix W_{CW} is constructed as the 625 rows of W_{TR} corresponding to m_0 . An ART algorithm is used to retrieve fluorescence local concentrations. The relaxation parameter is set to 0.1, the number of iterations is set to 200 for reconstructions in the TR case and to 600 for reconstructions in the CW case. In that way, the algorithm runs the same number of equations in the TR and in the CW case. An example of TR and CW reconstructed fluorescence is given in Fig. 2.

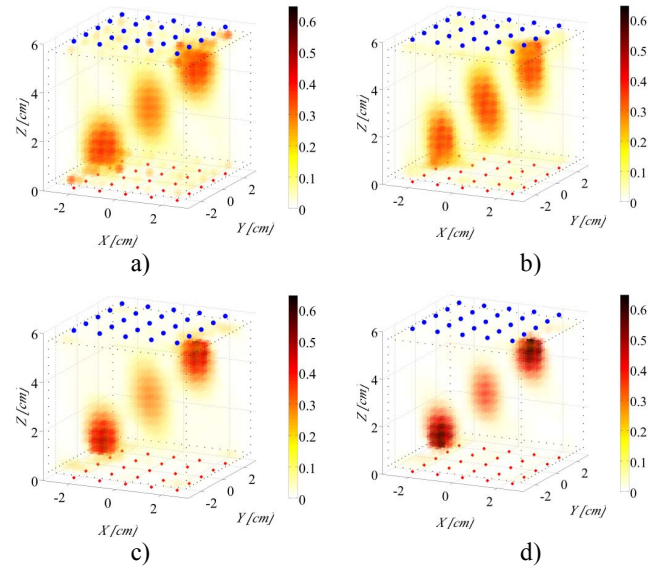


Fig. 2. Reconstructions of fluorescence markers concentrations in a medium where $n=1.4$, $\mu_a=0.04$ cm⁻¹, $\mu'_s=20$ cm⁻¹ and $\tau=0.3$ ns (a) CW; (b) TR with m_1 only; (c) TR with m_2 only; (d) TR with m_0 , m_1 and m_2 . Blue dots represent detector points and red crosses source points.

3.3. Distance of fluorescence

Here is introduced a parameter that we call the distance of fluorescence d_F . This distance is defined as the mean travel distance of photons within the medium, during a time equal to the fluorescence lifetime τ . For a homogeneous infinite medium, d_F is reduced to the simple expression:

$$d_F = 2\tau \frac{c}{n} \sqrt{\mu_a D}, \quad (6)$$

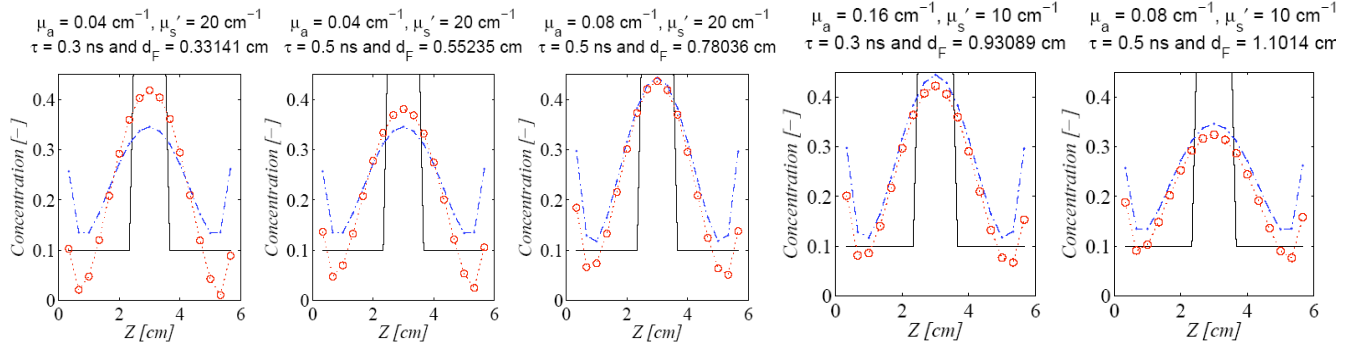


Fig. 3. Profile of reconstructed fluorescence markers concentrations of the central inclusion along the Z axis. The phantom concentrations are represented in full line, the CW concentrations in dashed line and the TR concentrations in dotted line.

This parameter self-consistently accounts for optical properties of the phantom and for the fluorescence lifetime.

4. RESULTS AND DISCUSSION

CW and TR reconstructions for phantoms with different optical properties and lifetimes are presented. Fig. 3 synthesizes the profiles of the reconstructed fluorescence concentrations for increasing d_F . It can be observed that TR reconstructions are of better quality than CW when d_F is smaller than 0.78 cm. On the other hand, when d_F is higher than 0.93 cm, there is no more benefit in using the TR method. More generally, the lower d_F is, the more the TR reconstruction is advantageous over the CW reconstruction. That conclusion is also observed for the profiles obtained for the two other inclusions (results not shown).

It seems that d_F , combining the three parameters τ , μ_a and μ_s' is a robust criterion to assess the potential benefits of the TR method. To sum it up, the TR method is *a priori* advantageous over the CW method when: i) the lifetime τ is short, ii) the medium is weakly absorbing, iii) the medium is highly diffusive.

ACKNOWLEDGMENT

This work has been supported by the Région Rhône-Alpes in the context of project I3M 'Multiscale Medical Imaging and modeling: from the small animal to the human being' of cluster ISLE.

REFERENCES

- [1] A. Yodh and B. Chance, "Spectroscopy and imaging with diffusing light," *Phys. Today*, vol. 48, no. 3, pp. 34–40, Mar. 1995.
- [2] R. Weissleder, "A clearer vision for in vivo imaging," *Nat Biotechnol*, vol. 19, no. 4, pp. 316–317, Apr 2001.
- [3] I. L. Medintz, H. T. Uyeda, E. R. Goldman, and H. Mattoussi, "Quantum dot bioconjugates for imaging, labelling and sensing," *Nat Mater*, vol. 4, no. 6, pp. 435–446, Jun 2005.

- [4] E. M. Sevick-Muraca and C. L. Burch, "Origin of phosphorescence signals reemitted from tissues," *Opt. Letters*, vol. 19, no. 23, pp. 1928–1930, Dec. 1994.
- [5] J. Wu, L. Perelman, R. R. Dasari, and M. S. Feld, "Fluorescence tomographic imaging in turbid media using early-arriving photons and laplace transforms," *Proc Natl Acad Sci U S A*, vol. 94, no. 16, pp. 8783–8788, Aug 1997.
- [6] X. Intes, V. Ntziachristos, J. P. Culver, A. Yodh, and B. Chance, "Projection access order in algebraic reconstruction technique for diffuse optical tomography," *Phys Med Biol*, vol. 47, no. 1, pp. N1–10, Jan 2002.
- [7] F. Gao, H. J. Zhao, Y. Tanikawa, and Y. Yamada, "A linear, featureddata scheme for image reconstruction in time-domain fluorescence molecular tomography," *Opt. Express*, vol. 14, no. 16, pp. 7109–7124, Aug. 2006.
- [8] A. Laidevant, A. Da Silva, M. Berger, J. Boutet, J. Dinten, and A. C. Boccara, "Analytical method for localizing a fluorescent inclusion in a turbid medium," *Applied Optics*, vol. 46, no. 11, pp. 2131–2137, Mar. 2007.
- [9] A. Liebert, H. Wabnitz, J. Steinbrink, H. Obrig, M. Moller, R. Macdonald, A. Villringer, and H. Rinneberg, "Time-resolved multidistance near-infrared spectroscopy of the adult head: intracerebral and extracerebral absorption changes from moments of distribution of times of flight of photons," *Appl Opt* 43, 3037–3047 (2004).
- [10] S. Lam, F. Lesage, and X. Intes, "Time domain fluorescent diffuse optical tomography: analytical expressions," *Opt. Express*, vol. 13, no. 7, pp. 2263–2275, Apr. 2005.
- [11] R. Pierrat, L. J. Greffet, and R. Carminati, "Photon diffusion coefficient in scattering and absorbing media," *J Opt. Soc. Am. A* vol. 23, pp. 1106–1110, 2006.
- [12] S. R. Arridge, M. Cope, and D. T. Delpy, "The theoretical basis for the determination of optical pathlengths in tissue: temporal and frequency analysis," *Phys Med Biol*, vol. 37, no. 7, pp. 1531–1560, Jul 1992.